

## **Centrifuge Modeling of Cone Penetration Testing in Layered Soil**

**Mohammad Khosravi, Ph.D.,<sup>1</sup> Ross W. Boulanger, Ph.D., F.ASCE,<sup>2</sup> Jason T. DeJong, Ph.D., M.ASCE,<sup>3</sup> Ali Khosravi, Ph.D.,<sup>4</sup> Masoud Hajialilue-Bonab, Ph.D.,<sup>5</sup> and Daniel W. Wilson, Ph.D., M.ASCE.<sup>6</sup>**

<sup>1</sup> Department of Civil and Environmental Engineering, University of California, Davis, CA, 95616, USA, khosravi@vt.edu

<sup>2</sup> Department of Civil and Environmental Engineering, University of California, Davis, CA, 95616, USA, rwboulanger@ucdavis.edu

<sup>3</sup> Department of Civil and Environmental Engineering, University of California, Davis, CA, 95616, USA, jdejong@ucdavis.edu

<sup>4</sup> Department of Civil and Environmental Engineering, Sharif University of Technology, Tehran, Iran; e-mail: khosravi@sharif.edu.

<sup>5</sup> Department of Civil Engineering, University of Tabriz, Tabriz, Iran, hajialilue@tabrizu.ac.ir

<sup>6</sup> Department of Civil and Environmental Engineering, University of California, Davis, CA, 95616, USA, dxwilson@ucdavis.edu

### **ABSTRACT**

The effect of soil interlayering on the measured cone penetration resistance was examined in a layered soil model tested on a 9-m radius centrifuge. The soil profile consisted of a layer of sand between overlying and underlying layers of low plasticity clayey silt. The sand layer thickness varied from 0 to 240 mm (model scale) along the length of the model. The sand was loose with a relative density of 44% on one side of the model, and dense with a relative density of 88% on the other side. The clayey silt had a plasticity index (PI) of 6 and over-consolidation ratio (OCR) of about 1.5. Multiple cone penetration soundings were performed along the width and length of the model using cone penetrometers with diameters of 4, 6 and 10 mm. The model construction procedure, data processing, and cone penetration testing results are described.

### **INTRODUCTION**

The cone penetration test (CPT) is a common site investigation tool due to the continuous measurements obtained during vertical penetration. It is particularly effective for delineating stratigraphic variations, including the detection of relatively thin layers. However, the cone tip resistance, sleeve friction, and pore pressure measurements are influenced by the strength, stiffness, and permeability of soils within an influence zone about 10 to 30 cone diameters from the cone tip. For this reason, the interpretation of cone penetration resistance in thinly interbedded soils or across interfaces between weaker and stronger soils should account for the influence of the other soils present within the zone of influence of the cone tip.

Cone penetration resistances in layered sand, layered clay, and layered sand and clay have been studied using chamber and small-scale model tests (Treadwell 1976, Meyerhof and Sastry 1978, Hird et al. 2003, Mlynarek et al. 2012, Tehrani et al. 2018), centrifuge model tests (Silva and Bolton 2004, Mo et al. 2015), analytical approaches (e.g., Vreugdenhil et al. 1994), cavity



expansion analyses (e.g., Xu and Lehane 2008), and axisymmetric penetration analyses (e.g., van den Berg et al. 1996, Ahmadi and Robertson 2005). These studies show that the cone penetration resistance in layered soils can depend on the cone diameter to particle size ratio, the layer thickness to cone diameter ratio, and the relative strength and stiffness of successive layers.

This paper summarizes the results of a centrifuge model test examining cone penetration resistance for a layer of sand between overlying and underlying layers of clayey silt. The sand was loose with a relative density ( $D_r$ ) of 46% on one side of the model, and dense with a  $D_r$  of 88% on the other side. The clayey silt had a plasticity index (PI) of 6 and over-consolidation ratio (OCR) of about 1.5. The sand layer thickness varied from 0 to 240 mm (model scale) over its length. Cone penetration resistances were measured using penetrometers with cone diameters ( $d_c$ ) of 4 mm, 6 mm, and 10 mm. The centrifuge model, construction procedure, cone penetrometer equipment, and testing program are described in detail. Representative tip resistance profiles from cone penetration soundings on the dense sand ( $D_r = 88\%$ ) side of the model are presented to illustrate a number of different effects. The results of the experiments and analyses provide insights on the effect of layering on the cone penetration resistance and an archived dataset for evaluating design procedures and numerical analysis methods.

## CENTRIFUGE TEST PROGRAM

A centrifuge test was performed using the 9-m radius centrifuge at the University of California at Davis. The test was performed in a flexible shear beam container at a centrifugal acceleration of 40g. The inner dimensions of the container in model scale were 1,651 mm long (66.0 m in prototype), 787 mm wide (31.5 m in prototype), and 580 mm tall (23.2 m in prototype). The recorded data and model dimensions were converted into prototype units according to the scaling laws described by Kutler (1995). All data are presented in model units unless otherwise specified.

The soil profile consisted of a layer of sand sandwiched between two layers of low plasticity clayey silt as shown in Figure 1. The sand and upper clayey silt layers varied in thickness along the length of the model container from about 0 to 240 mm. The thickness of the lower clayey silt layer was 210 mm. The centrifuge model had loose sand ( $D_r \approx 46\%$ ) on one side (over a width of 270 mm) and dense sand ( $D_r \approx 88\%$ ) on the other side (over a width of 518 mm). The sand layer was comprised of Ottawa (F-65) sand with a maximum void ratio ( $e_{max}$ ) of 0.83, minimum void ratio ( $e_{min}$ ) of 0.51, and median grain size ( $D_{50}$ ) of 0.2 mm (Parra Bastidas et al. 2017). Crushed, non-plastic silica flour (SIL-CO-SIL 250) and kaolin clay (Old Hickory No. 1 Glaze) were blended at a ratio of 4:1 by dry mass to create the clayey silt mixture with a PI of 6, Liquid Limit (LL) of 22, and coefficient of consolidation ( $C_v$ ) of about 2.4 mm<sup>2</sup>/s in normally consolidated loading (Price et al. 2017). A 40 mm-thick saturated dense coarse sand ( $D_r \approx 90\%$ ) was placed below the bottom clayey silt layer to provide drainage. Water was used as the pore fluid, and the water table was about 40 mm above the surface of the model.

The upper and lower clayey silt layers were placed as slurries and then consolidated in-flight. The clayey silt slurry was batch-mixed in a vacuum mixer at an initial water content of approximately 45% ( $\sim 2.0 \times LL$ ). The lower layer of clayey silt was placed as a single lift of slurry in the container. The container was mounted on the centrifuge and spun at a centrifugal acceleration of 60 g until the clayey silt was fully consolidated. The container was removed from the arm and excess clayey silt carved out using a spatula leaving a final layer thickness of 210 mm (Figure 2a). The clayey silt layer was kept wet during this process using a water sprayer. A thin layer of colored sand was pluviated over the clayey silt layer. A thin sheet of metal was placed



vertically at the location of the planned interface between the dense and loose sand zones as shown in Figure 2b. The loose and dense sand zones were constructed using dry pluviation, and then carefully vacuumed to their final thicknesses. The upper clayey silt layer was then slowly poured as a slurry over the sloped sand layer and the model with all layers of soils was again consolidated in-flight at the centrifugal acceleration of 60g. The centrifugal acceleration was reduced to 40g for the remainder of the test, such that all soils had an over-consolidation ratio of about 1.5. Figure 2d shows the soil model, cone penetrometer, and container on the centrifuge arm before testing.

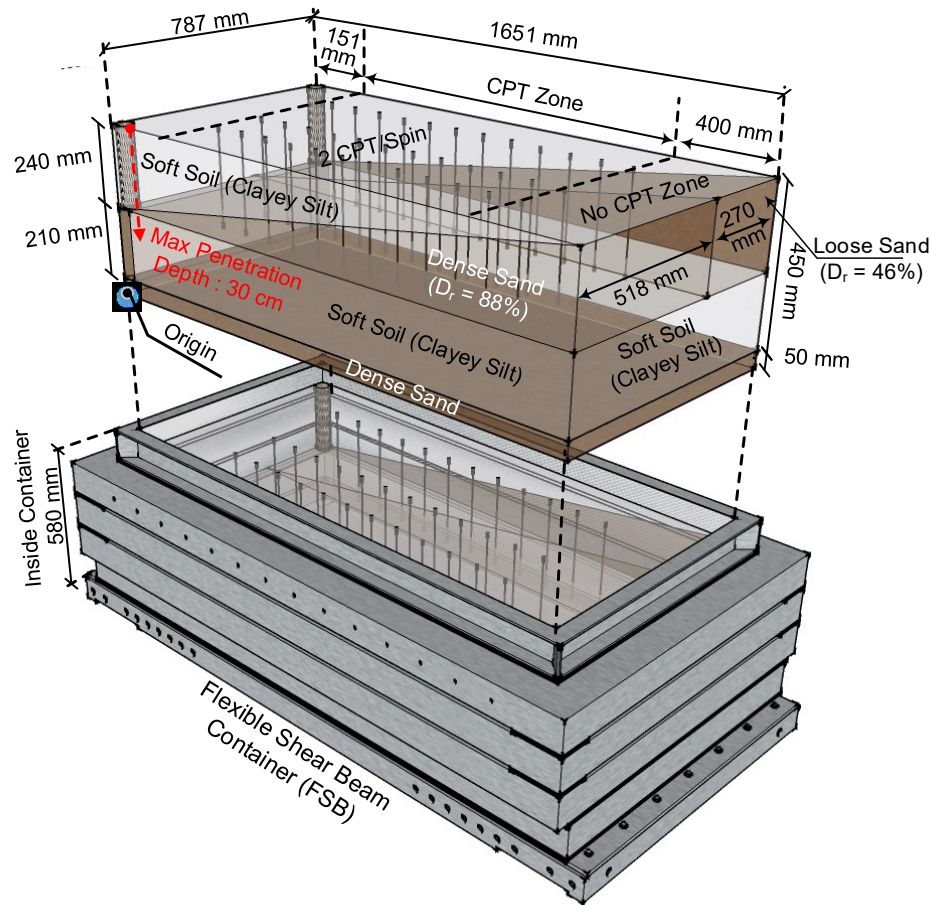


**Figure 1. Centrifuge model MKH05 stratigraphy and cone penetration test locations**

Cone penetrometers with outer diameters of 4, 6 and 10 mm and conical tip angles of 60° were used in this study. The ratio of the cone diameter ( $d_c$ ) to the median grain size ( $D_{50}$ ) of the soil ( $d_c / D_{50}$ ) for the three cones were 20, 30 and 50. Bolton et al. (1999) suggested that a  $d_c / D_{50}$  ratio of 20 or greater is sufficient to minimize particle size effects, which suggests that particle size effects would not be expected for the three cones used in this study. As shown in Figure 3, all three cone penetrometers had a load cell at the top to measure the total penetration resistance (i.e., tip resistance plus shaft resistance). Cone penetrometers with 6-mm and 10-mm diameters also had a load cell behind the cone tip (Figure 3) to directly measure the tip resistance. The recordings of the tip resistance for the 4-mm-diameter cone was estimated using the shaft friction measurements from the 10-mm-diameter cone, as discussed in detail in the next section. The 6-mm cone had a friction reducer ring 100 mm above the tip such that its shaft friction would be different from that for the other cones. Cone penetration tests were performed along the length (X dimension) and



width (Y dimension) of the model at the locations shown in Figure 1; locations are identified by the X-Y coordinates relative to the container corner labeled as the "origin".



**Figure 2. Model construction:** (a) carving the lower layer of clayey silt to its final thickness, (b) placing the metal sheet separating the dense and loose sand zones, (c) dry pluviator of sand layers, and (d) cone penetrometer and model on the centrifuge arm.

## DATA PROCESSING

**Penetration resistance in clayey silt layer.** The measured cone tip resistances ( $q_c$ ) in the clayey silt layer (Figure 4) were evaluated against expected ranges for tip resistance given undrained shear strengths data for this soil and the model's known stress history. The tip resistances measured with the 6-mm and 10-mm diameter cones were consistent with each other, and increased from zero near the surface to about 0.55 MPa at a model depth of 200 mm. The tip resistance can be estimated from the undrained shear strength ( $S_u$ ) using,

$$q_c = N_K S_u + \sigma_v \quad (1)$$

where  $\sigma_v$  is the in-situ overburden total stress, and  $N_K$  is the cone factor that varies between 11 and 19 with an average of 15 (Lunne et al. 1997). Based on Ladd and Foott (1974), the relationship between  $S_u/\sigma'_v$  and over-consolidation ratio (OCR) can be expressed as,

$$\left(\frac{S_u}{\sigma'_v}\right)_{OCR} = S \times (OCR)^m \quad (2)$$



where  $S$  is the value of  $S_u/\sigma'_v$  for normally consolidated soil and  $m$  is an exponent. Undrained monotonic direct simple shear tests on the clayey silt by Price et al. (2017) indicate  $S = 0.16$  and  $m = 0.75$ . Profiles of estimated tip resistance for  $N_k$  values of 11, 15, and 19 and undrained shear strength ratios for an OCR of 1.5 are shown in Figure 4, along with the  $q_c$  measured using the 6-mm and 10-mm cones. The measured  $q_c$  profiles are consistent with an  $N_k$  of 11 at depths less than about 75 mm and transition to being consistent with an  $N_k$  of about 17 at a depth of about 200 mm.

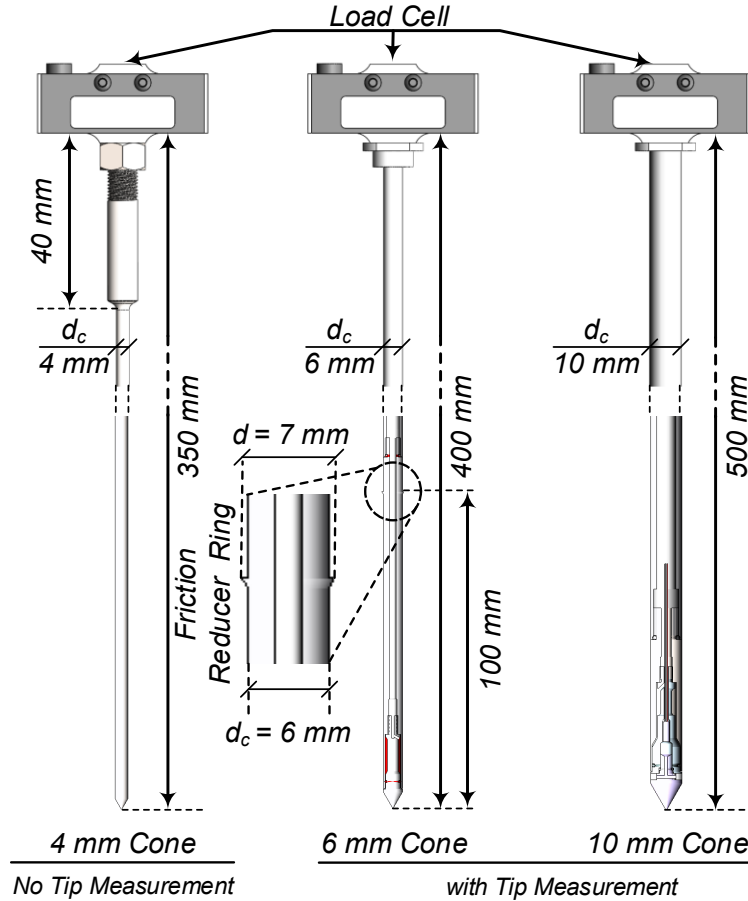


**Figure 3. Configurations of the three cone penetrometers.**

**Determining tip resistance for the 4-mm diameter cone.** The 4-mm diameter cone only measured the total penetration load ( $P_{tot}$ ) using the external load cell positioned above the ground surface. Therefore, the tip load ( $P_c$ ) had to be estimated by subtracting an estimate of the shaft resistance ( $P_s$ ). Profiles of the total load,  $P_{tot-10mm}$ , and tip load,  $P_{c-10mm}$ , measured by the 10-mm cone in the dense side of the container at  $X = 1151$  mm (i.e., distance along the model length from the origin on Figure 5), where the sand layer thickness is 182 mm, are presented in Figure 6a. The shaft load of the 4-mm cone,  $P_{s-4mm}$ , was estimated by scaling the shaft load of the 10-mm cone as,

$$P_{s-4mm} = P_{s-10mm} \frac{A_{s-4mm}}{A_{s-10mm}} = (P_{tot-10mm} - P_{c-10mm}) \frac{A_{s-4mm}}{A_{s-10mm}} \quad (3)$$

where  $A_s$  is the embedded shaft surface area. Profiles of the measure total load,  $P_{tot-4mm}$ , and estimated shaft load of the 4-mm cone,  $P_{s-4mm}$ , are presented in Figure 6b. The tip load of the 4-mm cone can then be estimated by:

$$P_{c-4mm} = P_{tot-4mm} - P_{s-4mm} \quad (4)$$



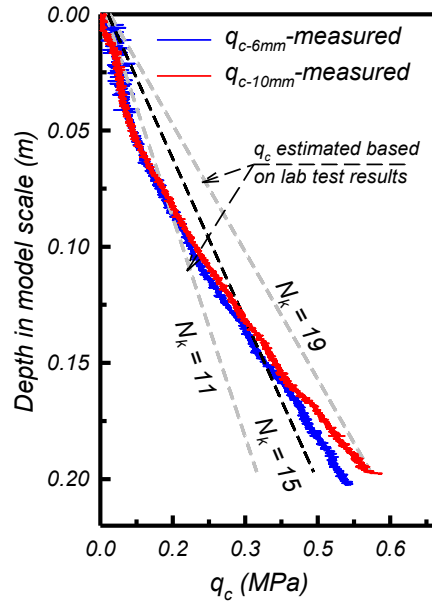


**Figure 4. Profiles of measured and estimated cone tip resistances in the clayey silt.**

as presented in Figure 6c. The estimated shaft load is typically 5-20% of measured total load throughout the sand layer, but becomes almost equal to the total load after the cone enters the underlying clayey silt layer. Thus, this approach for estimating tip resistance for the 4-mm cone is considered reasonable for the sand layer, but less reliable for the underlying clayey silt layer.

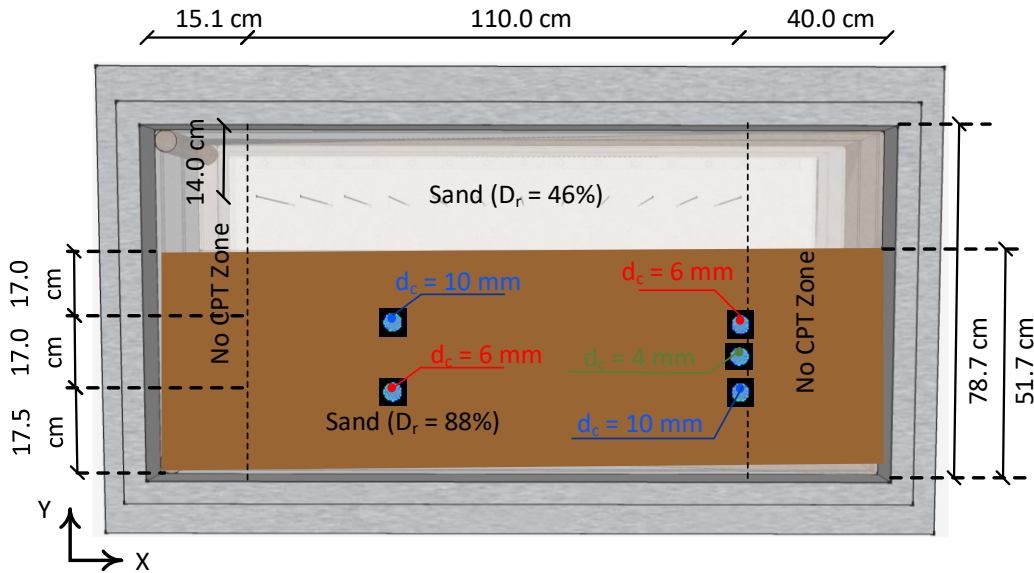


**Figure 5. Locations of the cone penetration soundings presented later.**



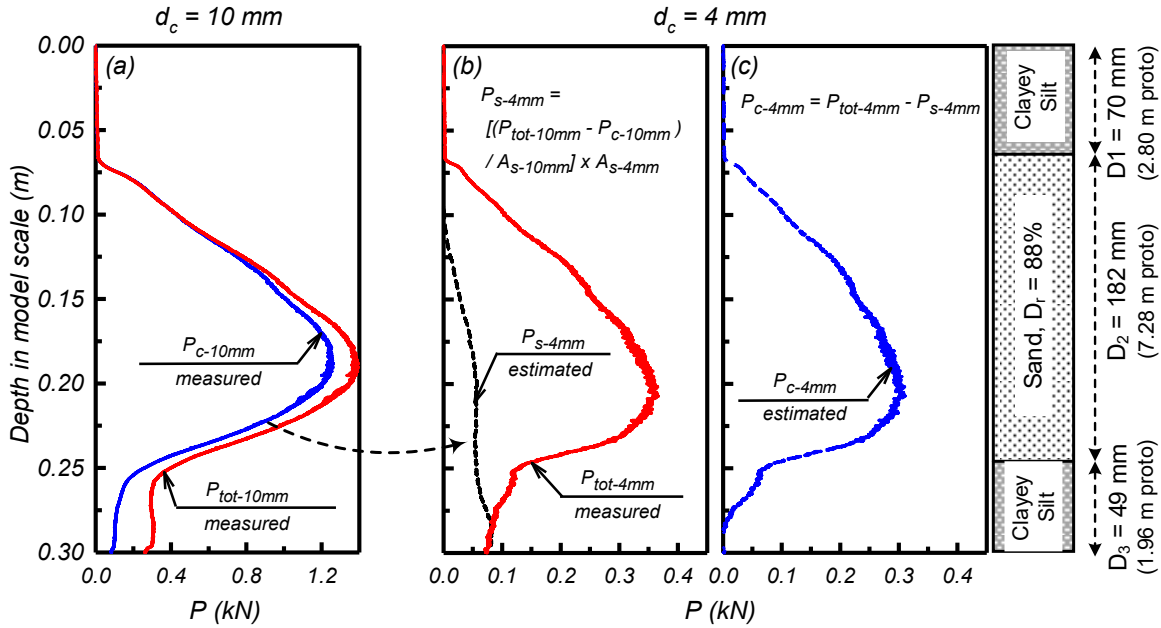


**Figure 6. Profiles of tip and total penetration loads in the dense sand: (a) measured loads by the 10-mm cone, (b) measured total load and estimated shaft load of the 4-mm cone, (c) estimated tip load of the 4-mm cone at one location along the model length.**

## CONE PENETRATION RESULTS

Profiles of tip resistance from cone penetration soundings on the dense sand ( $D_r = 88\%$ ) side of the model are plotted in Figure 7. The results include the tip resistance from cones with  $d_c = 4, 6$  and  $10$  mm at two different locations of the model:  $X = 482$  mm with the sand layer thickness of  $80$  mm ( $3.20$  m in prototype) in Figure 7a, and  $X = 1151$  mm with the sand layer thickness of  $182$  mm ( $7.26$  m in prototype) in Figure 7b. These data illustrate the influence of the cone diameter on the measured tip resistances across the range of layer thicknesses present in the model. Tip resistances are small in the overlying clayey silt, but begin to increase when the cone tip is positioned about 1 to 2 cone diameters above the top of the dense sand layer. Tip resistances progressively increase with depth in the dense sand layer until the cones begin to sense the lower clayey silt layer, after which the tip resistances progressively reduce as the cones approach the top of the clayey silt layer. The distance between the top of the clayey silt layer and the depth where the tip resistance peaked in the dense sand is labelled as the sensing distance,  $d_s$  (Figure 7). The value of  $d_s$  depends on the cone diameter and the sand layer thickness. For the location where the sand layer thickness was  $80$  mm (Figure 7a), the sensing distance ranges from 5 cone diameters for the  $10$ -mm cone to 10 cone diameters for the  $4$ -mm cone. For the location where the sand layer thickness was  $182$  mm (Figure 7b), the sensing distance was about 6 cone diameters for the  $10$ -mm cone and 12 cone diameters for the  $4$ -mm cone.

The peak cone tip resistances in the sand layer reflect the influence of the overlying and underlying clayey silt layers. As the thickness of the sand layer increased from  $80$  mm (Figure 7a) to  $182$  mm (Figure 7b), the peak tip resistance increased by  $38\%$  for the  $4$ -mm cone,  $55\%$  for the  $6$ -mm cone, and  $73\%$  for the  $10$ -mm cone. For the  $80$  mm thick sand layer (Figure 7a), the ratio of sand layer thickness to cone diameter ( $D_2/d_c$ ) was  $20, 13$ , and  $8$  for the  $4$  mm,  $6$  mm, and  $10$ -mm cones, respectively, all of which are insufficient for mobilizing a "true" tip resistance. The trend



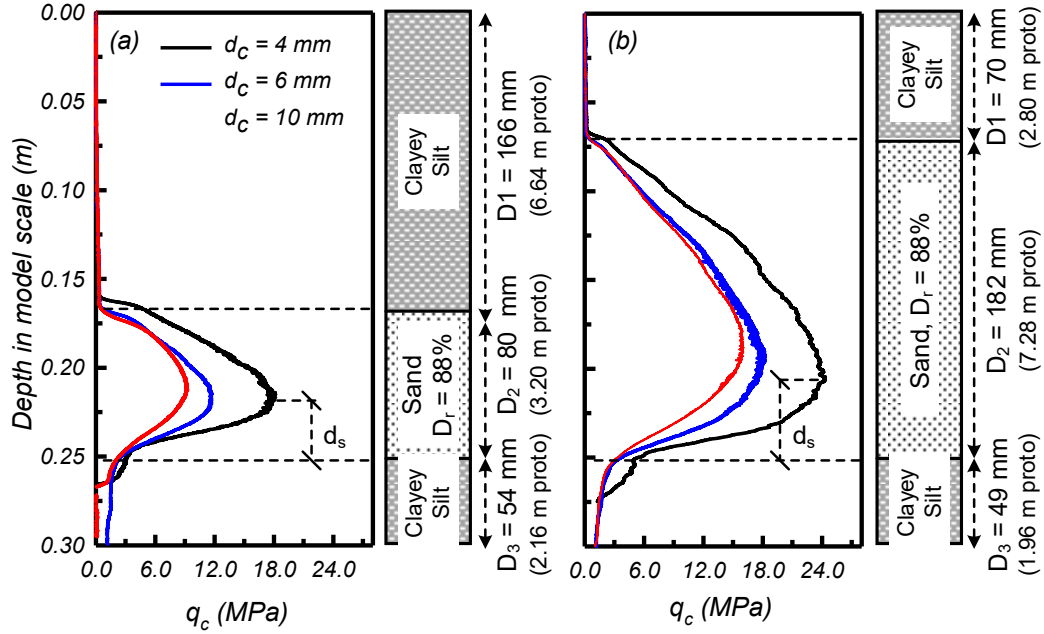


**Figure 7. Profiles of penetration resistance in the dense side of the container for cone penetrometers with  $d_c = 4$  mm, 6 mm, and 10 mm at  $X = 482$  mm and 1151 mm.**

of decreasing tip resistance with increasing cone diameter in the 80-mm-thick dense sand layer is attributable to the greater influence of the clayey silt layers as  $D_2/d_c$  decreases from 20 to 8. For the sand layer thickness of 182 mm (Figure 7b), the  $D_2/d_c$  ratio was 46, 30, and 18 for the 4 mm, 6 mm, and 10-mm cones, respectively. The tip resistances are less affected by cone diameter for the 182-mm-thick sand layer, which is attributable to less of an influence of the clayey silt layers for this range of  $D_2/d_c$  ratios. These observations are consistent with the results presented in previous studies (e.g. Ahmadi and Robertson 2005, Xu and Lehane 2008).

The maximum value of the overburden corrected tip resistance ( $q_{c1N,max}$ ) in the dense sand layer is plotted versus the cone diameter to median grain size ratio ( $d_c/D_{50}$ ) for these two sand layer thicknesses in Figure 7. The overburden corrected tip resistance was computed by:

$$q_{c1N} = \frac{q_c}{P_a} \left( \frac{P_a}{\sigma'_v} \right)^{0.5} \quad (5)$$

where  $P_a$  is the atmospheric pressure (Liao and Whitman 1986). Previous studies have indicated that a  $d_c/D_{50}$  ratio of 20 or greater is required for minimizing any dependence of  $q_c$  on cone diameter (also referred to as a particle size effect) (e.g., Bolton et al. 1999). The trend of  $q_{c1N,max}$  decreasing with increasing  $d_c/D_{50}$  in Figure 8 are suggestive of a particle size effect, but this trend may be largely due to the influence of the clayey silt layers for this range of  $D_2/d_c$  ratios, plus uncertainty in the procedure used to estimate tip resistances from total load measurements with the 4-mm cone. For example, the  $q_{c1N,max}$  in the 182-mm-thick sand layer was only about 8% smaller with the 10-mm cone ( $D_2/d_c = 18$ ,  $d_c/D_{50} = 50$ ) than with the 6-mm cone ( $D_2/d_c = 30$ ,  $d_c/D_{50} = 30$ ), which is more likely attributable to the smaller  $D_2/d_c$  ratio (18 versus 30) than to a particle size effect ( $d_c/D_{50} = 50$  versus 30). At this same location, the  $q_{c1N,max}$  with the 4-mm cone was about 30% greater than with the 6-mm cone, which may be partly attributed to the greater  $D_2/d_c$  ratio (46 versus 30), the smaller  $d_c/D_{50}$  ratio (20 versus 30), or uncertainties associated with estimating the tip resistance for the 4-mm cone from the total penetration load (Figure 5). The trends for the 80-



mm-thick sand layer show a stronger dependence on cone diameter, which is attributed to the smaller range of  $D_2/d_c$  ratios (8 to 20). Thus, the observed effects of cone diameter on penetration resistance are believed to predominantly reflect layer thickness effects, with a smaller contribution of particle size effects for the 4-mm cone.

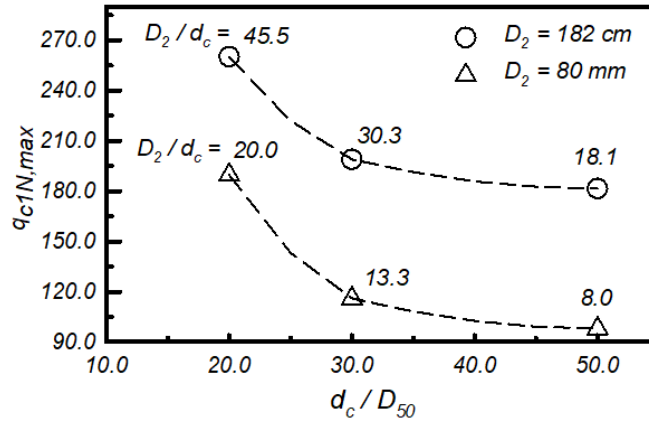


**Figure 8. Variation in tip resistance with cone diameter and sand layer thickness**

## CONCLUSION

The effect of soil interlayering on cone penetration resistance was examined in a centrifuge model test on a 9-m radius centrifuge. The soil profile consisted of a layer of sand between overlying and underlying layers of low plasticity clayey silt. The sand layer varied in thickness along the model length and was loose on one side and dense on the other side. Cone penetration tests were conducted using penetrometers with diameters of 4, 6 and 10 mm. The model construction procedure and aspects of the data processing were described.

Representative tip resistance results from cone penetration soundings on the dense sand ( $D_r = 88\%$ ) side of the model illustrate the dependence of measured tip resistances on the cone diameter, sand layer thickness and strength properties of the soil on either side of the layer interfaces. In the sand, the tip resistance was influenced by the underlying clayey silt at sensing distances of 5-12 cone diameters. The effects of cone diameter on tip resistance were attributed primarily to the ratio of sand layer thickness to cone diameter (i.e., thin layer effects), but may also reflect an influence of the ratio of cone diameter to median particle size (i.e., particle size effects) and uncertainty in determining the tip resistance for the 4 mm diameter cone from an above-ground total force measurement. The full set of cone penetration tests in this model are currently being processed and will be used to further examine the above described effects.

## ACKNOWLEDGEMENTS

This material is based upon work supported by the National Science Foundation (NSF) under grants CMMI-1300518 and CMMI-1635398. Operation of the centrifuge facility at the University of California at Davis was supported as part of the Natural Hazards and Engineering Research Infrastructure (NHERI) network under NSF award CMMI- 1520581. Any opinions, findings, and conclusions or recommendations expressed in this material are those of the authors and do not necessarily reflect the views of the National Science Foundation. The authors appreciate the assistance of the staff of the Center for Geotechnical Modeling at UC Davis.



## REFERENCES

- Ahmadi, M. M. and Robertson, P. K. (2005). "Thin-layer effects on the CPT qc measurement." *Can. Geotech. J.*, 42(5), 1302-1317.
- Bolton, M. D., Gui, M. W., Garnier, J., Corte, J. F., Bagge, G., Laue, J. and Renzi, R. (1999). "Centrifuge cone penetration tests in sand." *Geotechnique*, 49(4), 543-552.
- Hird, C. C., Johnson, P., and Sills, G. C. (2003). "Performance of miniature piezocones in thinly layered soils." *Géotechnique*, 53(10), 885-900.
- Kutter, B. L., (1995). "Recent Advances in Centrifuge Modeling of Seismic Shaking (State-of-the-Art Paper)." *Proc. of 3rd Int. Conf. on Recent Advances in Geotechnical Earthquake Engineering and Soil Dynamics*, 2, 927-942.
- Ladd, C. C., and Foot, R. (1974). "New design procedure for stability of soft clays." *J. of the Geotech. Eng. Div.*, 100(7), 763-786.
- Liao, S. C., and Whitman, R. V. (1986). "Overburden correction factors for SPT in sand." *J. Geotechnical Engineering*, ASCE, 112(3), 373-377.
- Lunne, T., Robertson, P.K., and Powell, J.J.M. (1997). *Cone Penetration Testing in Geotechnical Practice*. Blackie Academic/Routledge Publishing, New York.
- Meyerhof, G. G. and Sastry, V. V. R. N. (1978). "Bearing capacity of piles in layered soils. Part 1. Clay overlying sand." *Can. Geotech. J.*, 15(2), 171-182.
- Mlynarek, Z., Gogolik, S., and Poltorak, J. (2012). "The effect of varied stiffness of soil layers on interpretation of CPTU penetration characteristics." *Archives of Civil and Mechanical Engineering*, 12, 253-264.
- Mo, P. Q., Marshall, A. M., and Yu, H. S. (2015). "Centrifuge modelling of cone penetration tests in layered soils." *Geotechnique*, 65(6), 468-481.
- Parra Bastidas, A. M., Boulanger, R. W., DeJong, J. T., and Price, A. B. (2017). "Effects of pre-strain history on the cyclic resistance of Ottawa F-65 sand." 16th World Conference on Earthquake Engineering, 16WCEE, Santiago, Chile, January 9-13, paper 1213.
- Price, A. B., DeJong, J. T., and Boulanger, R. W. (2017). "Cyclic loading response of silt with multiple loading events." *Journal of Geotechnical and Geoenvironmental Engineering*, ASCE, 2017, 143(10): 04017080, 10.1061/(ASCE)GT.1943-5606.0001759.
- Silva, M. F. and Bolton, M. D. (2004). "Centrifuge penetration tests in saturated layered sands." *Proc. of the sec. Int. Conf. on site characterization*, ISC-2, 1, 377-384. Rotterdam, the Netherlands: Millpress.
- Tehrani, F. S., Arshad, M. I., Prezzi, M., and Salgado, R. (2018). "Physical modeling of cone penetration in layered sand." *Journal of Geotechnical and Geoenvironmental Engineering*, 144(1), 04017101.
- Treadwell, D. D. (1976). "The influence of gravity, prestress, compressibility, and layering on soil resistance to static penetration." *PhD thesis*, University of California at Berkeley, Calif.
- van den Berg, P., de Borst, R. & Huetink, H. (1996). "An Eulerian finite element model for penetration in layered soil." *Int. J. Numer. Analyt. Methods Geomech.*, 20(12), 865-886.
- Vreugdenhil, R., Davis, R. & Berrill, J. (1994). "Interpretation of cone penetration results in multilayered soils." *Int. J. Numer. Analyt. Methods Geomech.*, 18(9), 585-599.
- Xu, X. T. and Lehane, B. M. (2008). "Pile and penetrometer end bearing resistance in two-layered soil profiles." *Geotechnique*, 58(3), 187-197.